Indian Journal of Geo Marine Sciences
Vol. 46 (08), August 2017, pp. 1673-1681

Experimental investigation of aerodynamic performances on a rotating cylinder with surface roughness using light weight smart motor (LWSM)

M.T. Abu Seman[1*], F.Ismail[2], M.Z. Abdullah[2] & M.N.A Hamid[3]

[1]Department of Mechanical, Polytechnic Seberang Perai, Permatang Pauh, Penang, Malaysia
[2]School of Aerospace Engineering, Universiti Sains Malaysia, Nibong Tebal, Penang, Malaysia
[3]Universiti Kuala Lumpur, Malaysian Spanish Institute, Kulim Hi-Tech Park, Kulim Kedah

[Email: mizie_edu@yahoo.com]

Received 28 January 2015 ; revised 30 October 2016

A critical adjustment was established by the attachment of the lightweight smart motor (LWSM) to an open circuit wind tunnel in order to determine lift and drag forces. LWSM rotated efficiently and the system can assemble and dissemble various cylinders with complete control, in comparison to other approaches available in the literature. The results of the experiment displayed accurate measurements of lift and drag. Research was performed with a free stream velocity of a wind tunnel within a range of $0.65<U\infty<13.21$ m/s for a flow over a two-dimensional rotating cylindrical object; with roughness variation at $5.0\mu m<Ra<77\mu m$ and circumferential velocity of the cylinder at range $0<\propto<6$ rad/s. It was found that the implementation of LWSM can measure forces in various rotating speed with less vibrating effect.

[Keywords: Circular cylinder, Surface roughness, Lift and drag coefficient, Friction force, Rotational rate.]

Introduction

In recent years, numerous approaches were considered and advanced, along with a few surveys by P.W. Bearman [1], E. Naudascher [2] and M. Griffin et al.[3] in order to govern the dynamics of the wake vortex by decreasing the magnitude of the varying lift and drag. The first factor determined the vibrations from a circular cylinder that was produced at a specific rotational rate, creating a vortex-induced vibration[4,5,6,7]. The increase in small amplitudes of drag was caused by the cylinder wake.

The second factor, investigated by Tokumaru and Dimotakis[8], was the flow control by the rotational cylinder; whereby, specific sequences of high force frequency and a large rotational amplitude was required to view a drag reduction and the ensuing flow management of the cylinder wake. It was discovered, in a 2D computational research by Mittal and Kumar[9], that the flow was stable when Re=1.91, and unstable between Re=4.3 - 4.8.

To determine the effects of a rotating cylinder upon the flow,[10] positioned a rotating cylinder near a wall where a flow of water was present, forming a 2D design, since a 3D layout would involve the axis of the cylinder (the vortex shedding) to be along the length of the wall.

The third factor focused on the rotational handling of the cylinder, involving research in experimental fluid dynamics. Previous experiments, by Satish et al.[11], yielded unsatisfactory results since a step circular cylinder was rotated and placed in a vertical trajectory. Another study by Gu et al.[12] applied a different experimental structure, whereby the use of splitter plates (connected to a fixed circular cylinder that did not rotate) was performing all the rotations instead. Moreover, Lam[13] conducted an investigation of a circular cylinder. However, the rotation of the cylinder was insufficient to aid in the perceptibility of the flow. They suggested to study of rotation cylinder in very low values of rotating rate as a foundation before proceed to high rotating rate. In addition, Jones et al.[14] mainly focused on the smooth cylinder without any surface roughness. Achenbach[15] and Nakamura et al.[16] assessed the cylinder with distributed roughness. Moreover, their research revolved around a fixed cylinder with no rotational movements and a high Reynolds number.

Most researchers measured the distribution around the cylinder by means of surface pressure tapes[17], and then obtained the mean force by combining them around the circumference. Shedden and Lin[18] used a laser-cantilever forces transducer to investigate the fluctuation in the drag force, while Sakamoto and Oiwake[19] used a strain-gauge balance to measure the mean and variable force. Since different diagnostic methods were used to conduct the experiments under different conditions with cylinder models having different degrees of stiffness, there were many inconsistencies in the experimental data, particularly with regard to the variable force. So and Savkar[20] used two piezoelectric three-axis load-cells to measure the average variable force exerted on a rigid cylinder across the span in a turbulent stream. Sin and So[21], Baban et al.[22], Baban and So[23], Fox and West[24,25] and West and Apelt[26] later used similar sensors to measure the variable forces since the piezoelectric load cell technique had the benefits of high resolution, small size and high degree of stiffness. Because of these advantages, K. Lam et al.[27] also suggested that this method be used to measure the immediate integral forces exerted on the circular cylinder.

Present study is to provide essential information in the field of aerodynamics by inspecting the management of the LWSM on the rotating circular cylinder, which yields accurate measurements of lift and drag. The high rotational rate was within a range of $0<\alpha<6$ rad/s for Reynolds number $2000<Re<43000$. This experiment herein is conducted to present solutions to certain perspectives that were not calculated and presented previously.

Materials and Methods

Cylinder Development

The summary of previous research investigations regarding the size of the cylinder used for rotation. Lam[28] and Badalamenti[29] was conducted previous studies with various cylinder diameter and cylinder length. They is presented 38.1mm and 88.9mm for diameter with length is 440mm and 450mm. However, they were presented the scope of study only in vortex shedding. Hence, in present study the average cylinder size was 50mm in diameter, with a length of 300mm. In this experiment, we were studied lift and drag as a scope of study. In order to obtain accurate results, scaling analysis was performed to efficiently imitate the cylinder, which may also contribute to the industry.

In four cylinder types, with varying surface roughness, used as instalments to the LWSM; contrary to previous studies conducted by them. The roughness profiles attached to a cylinder are cylinder A with 5.078 μm, cylinder B with 39.88 μm, cylinder C with 60.15 μm and cylinder D with 76.99 μm. All four cylinders were composed of hollow aluminium tubing. To achieve different surface roughness, various qualities of sand paper were adhered on the surface of each cylinder. The surface roughness of all four cylinders ranged from $5.0 < Ra < 77$, respectively.

The sand paper is measured using IF-Profiler surface roughness (Alicona IF-Profiler). The value of surface roughness depends on the scale of measurement. In addition, the concept roughness had statistical implications as it considers factors such as sample size and sampling interval. Three measurements at different locations on each sand paper were taken and the average of these three readings was recorded as the surface roughness value for each sand paper. Average surface roughness (R_a, in μm) of the specimens is determined with IF-Profiler. The output results of the instrument were determined by the average surface roughness by:

$$R_a = \frac{1}{L}\int_0^L |z(x)|dx \qquad [1]$$

where L is the length, z is height and x is distance along measurement.

The entire friction measurements were replicated three times and calculated as an average of total contact friction. The experiment is repeated for different rough cylinders. The friction force per length of pulley contact (N/m) on the smooth and rough cylinder represented as,

$$f_r = \frac{F_r}{\pi \mathrm{r}} \qquad [2]$$

where F_r is friction force and r radius of cylinder. The friction forces for smooth and rough cylinders are presented in Fig 1.

The F_r results for silicon carbide #36, #60 and #80 sandpaper which that this surface display significant roughness effect even at the lowest speed of rotation at starts to increase for higher RPM.

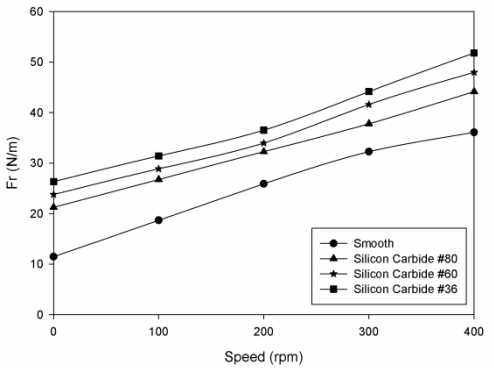

Fig.1 - Friction force (N/m) versus speed (rpm) for smooth and rough cylinders.

Light Weight Smart Motor (LWSM)

In order to measure the lift and drag forces, a lightweight motor smart motor has been developed. Along with the lightweight quality, the LWSM demanded a simplistic design, one that may be easily assembled when calculating the forces of aerodynamics. Furthermore, the LWSM was durable with precise joints that connected the motor to the cylinder, as shown in Fig 2. Its movement was devised to have minimum vibrations while rotating.

Two calibrations were performed in order to assess the readings from the rotations. The first calibration was performed prior to the assembly of the motor and cylinder to the wind tunnel. This involved the reduction of vibrations of specific points on the cylinder with the use of a magnetic gauge. The vibrations were significantly reduced to ±0.15mm, as shown in Fig 5. After fixing the motor and cylinder to the wind tunnel, a second calibration was carried out in which readings were documented; first without free stream velocity and second with free stream velocity. The difference of the recorded readings preceded each test.

The mount was constructed using a Teflon material which provided a firm grip on the cylinder, along with flexible mobility. To ensure a smooth rotation of the motor and cylinder, two differently sized ball bearings were utilised. Bearing was installed to support the weight of the cylinder, balance the motor while keeping the vibrations at a minimum. The main function of the motor was to deliver high speed and energy, with increased torque values. In order to specifically measure the lift and drag, balancing unit system.

Load cell

According to the ideas and methods of researchers, the calibration of the load cell is statistically performed by measuring the static calibration in the direction of the lift and drag. The applied force was a dead weight within the range of 0-6N, and the calibration was performed at three spots along the span of the cylinder. Once weight was applied to a cylinder, the values for lift and drag are taken from load cell reading display. The static calibration was repeated thrice before the average lift and drag was taken to obtain the most accurate value possible.

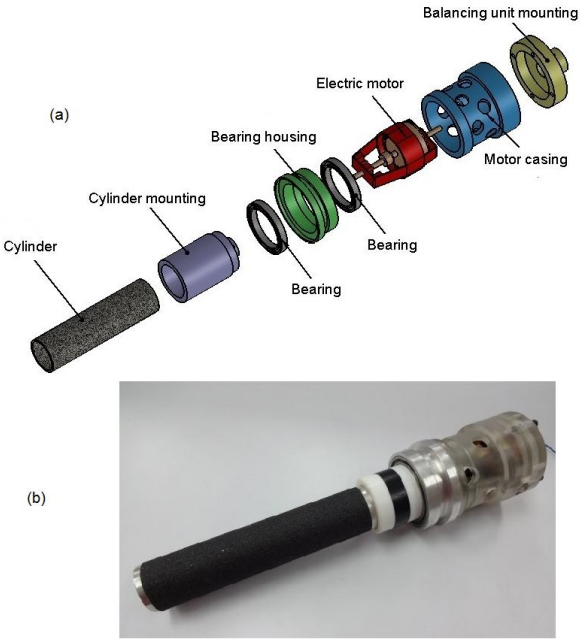

Fig.2 - (a) 3D Isometric view for LWSM components (b) Complete LWSM set

Experimental Setup and Procedures

The main goal of this study was to utilise the LWSM to calculate the forces of lift and drag; with the aid of the rotational circular cylinder that consisted of four different surface roughness, and a test section of an open-circuit wind tunnel that had a cross-sectional area of 300mm x 300mm. Additional items were also used to set up the experiment: a velocity controller, a computer, a force measurement system and a data acquisition unit; as shown in Fig 3. Moreover, the electronic speed variator of fans controlled the velocity within the test section of the wind tunnel. The maximum velocity was 36m/s.

The experiment was prepared by connecting the wind tunnel and the LWSM through the rotational circular cylinder. The LWSM was mounted on a balancing unit. As previously mentioned, the cylinder was composed of hollow

aluminium tubing. The external diameter was D=50mm. The surface of the cylinder may be altered with the use of numerous qualities of sand paper, acting as the surface roughness medium; as illustrated in Table 2. This set-up was convenient and time-efficient since the cylinders may be substituted with ease; without the readjustment of screws and bolts. To acquire precise lift and drag measurements, four beams were placed firmly in the shape of a parallelogram, with strain gages affixed on top of the beams and strain gage bridges connecting all four beams. This prevented any association between the forces acting on the lift and drag components and the rotating cylinder. The balance was designed to be free from the test section in order to eliminate internal damping effects.

The experimental procedure was summarised as shown in Fig 4. The collection of the vertical force by joining the signal from the load cell to the data acquisition board. The graphical user interface data acquisition software was installed in the computer. Four input channels were present; each had its own unique connection design.

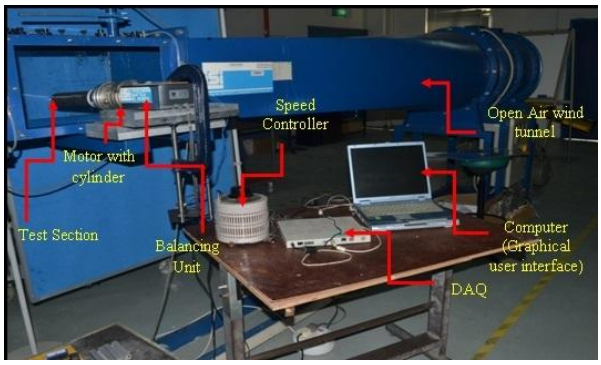

Fig.3 Open circuit wind tunnel

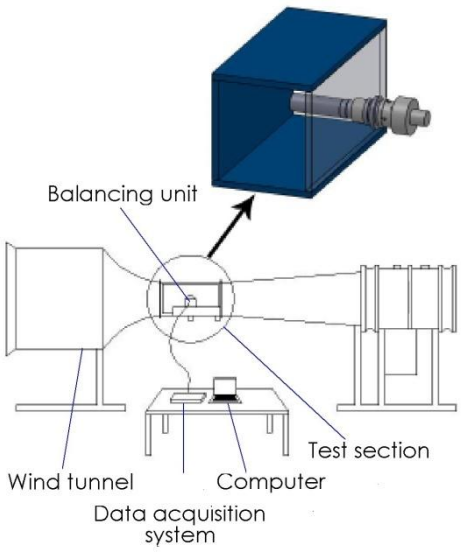

Fig.3 b) Schematic of the experimental setup

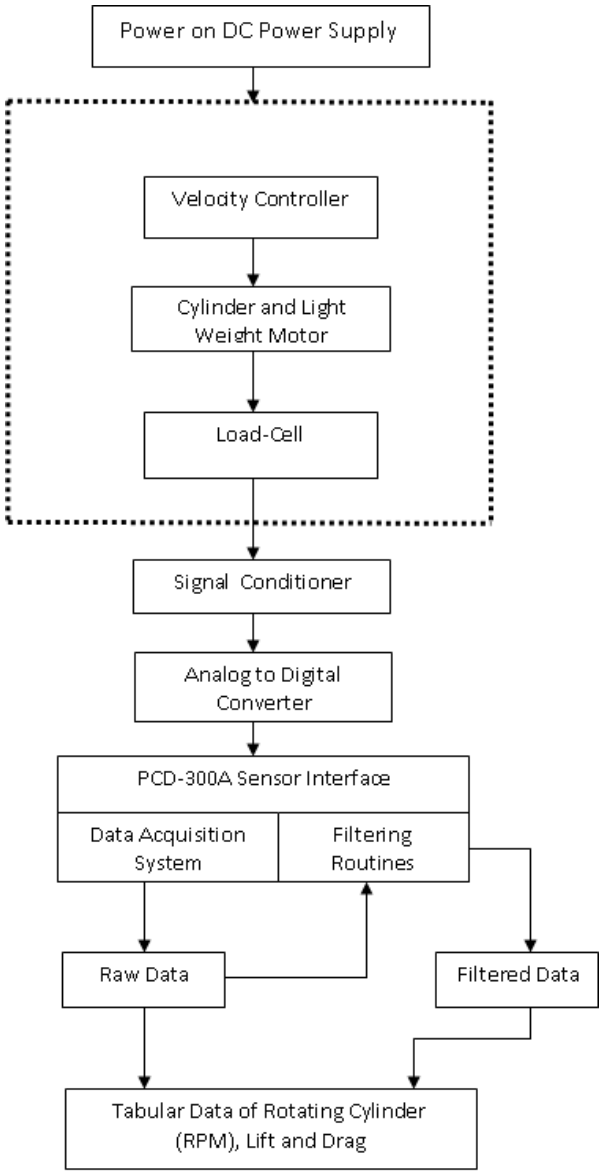

Fig.4 - Flow chart of the experimental procedure

Data acquisition software (Kyowa, PCD-300A Kyowa-Electronic Instruments Co, LTD, Tokyo, Japan) was set with a 10,000 μm/m range and an offset value of 1 and 0 calibration factors. From the full scale (5N), the force sensors had the precision of 0.3%. Load-cell's data breeding rate was set at 5000 points/s. For every fix and rotating cylinder condition, 50,000 points of data were chosen and unified into time-averaged lift and drag coefficients. Exact control over the rotation speed was accomplished, with the speed range between $0 \leq \alpha \leq 6$. In order to attain the free-stream velocities, previous identical experiments were reviewed and the values were decided to be within $U\infty$ =0.65 and $U\infty$ =13.21m/s. In the present study, the Reynolds number is range $2000<Re<43000$ which can be considered laminar and turbulence flow.

Dynamic Vibration

Almost every object that moves or rotates, cause a certain amount of vibrations. The frequency with flow indicates that the air flow moving through to the centre of cylinder surface in wind tunnel. Thus, the frequency without air flow is indicated during a cylinder is free of installation in wind tunnel. For this experiment, the vibration of the rotating cylinder in the LWSM was calculated in the range of 100<rpm<400, as illustrated in Table 1.

Table 1 - Rotating cylinder range

Rotation rate (rpm)	Freq. (Hz) without flow	Freq. (Hz) with flow
100	1.67	0.17<α<3.46
200	3.33	0.34<α<6.92
300	5.00	0.51<α<10.38
400	6.67	0.68<α<13.84

In order to confirm that the rotating motor was not in the natural frequency's range, the LWSM was assessed by the LMS test lab. Mode number is indicated the values of frequency on motor measurement. The values were displayed in Table 2.

Table 2 - Natural Frequency measurement on motor

Mode number	Frequency (Hz)
Mode 1	23.761
Mode 2	177.117
Mode 3	211.299

From the values shown in Table 4, it was confirmed that the LWSM's rotating cylinder was well out of the natural frequency range since its minimum and maximum frequency range were between 0.17<Hz<13.84. Minimum value for the natural frequency range was 23.761Hz. As previously mentioned, two calculations were made while operating the cylinder: one with wind flow velocity and one without. Furthermore, to fully assess the displacement vibration values and to ensure that they were in the minimum range, the amplitude of the rotating cylinder was measured by a laser displacement sensor, as presented in Fig 5.

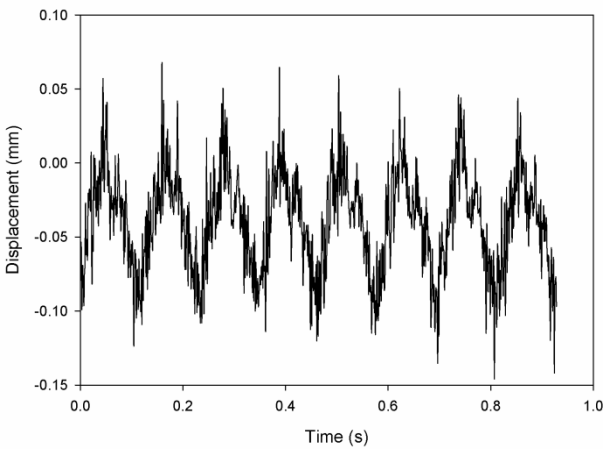

Fig.5- Displacement vibrations on LWSM

The acceleration (g) displacement in the 2D graph was dependent on the rotation of the cylinder. Minimum limit displacement was calculated to be ±0.15mm, as featured in the graph, and was a satisfactory value in regards to dynamic cases.

Results and Discussions

The experimental results herein for the two-dimensional circular cylinder quantitatively differs from the literature perhaps due to the variations in the set-up of the experimental conditions. These include the cylinder length to diameter ratio, the finishing condition of the models, the turbulence characteristics and in the case of a smooth cylinder and the degree of surface roughness.

The variation of the drag coefficients for non-rotating cylinder as a function of the Reynolds number has studied in past study. Experimental data is in qualitatively matches to the work of U.Butt et al.[30] where C_D value is 1.18 at Re=10000 and it's quite close with current study, C_D=0.9096 at Re=11000. In this experiment, they was used a cylinder size 156mm compared with current study is 200mm.

Coefficient of drag and lift forces on the rotating cylinder with different roughness

The experiment of four varieties of cylinder roughness with a rotation speed of 0 rpm was compared as shown in Fig 6(a) and was set as a benchmark for the next results. Next, in Fig 6(b) the experiment results with a rotation speed of 100 rpm. It was found that the C_D suddenly

decreased when the Re increased to Re<10000. This was followed by a continued rise in the drag between 10000< Re <14000, which then decreased and faded at Re>14000. Since the cylinder possessed a surface roughness, this had a consequential effect on the drag coefficient. The roughness caused an early transition to the critical, followed by an increase in the minimum C_D. Three cylinders with the most roughness corresponded to the drag coefficients reaching a common level in the transcritical range; this was in agreement with Achenbach[31].

As the rotational speed increased to 400 rpm, the drag coefficients slightly decreased; as displayed in Fig 6(c). In the initial phase of Re, the curves on the graph with speed 400 rpm looked quite similar to the curves that had a speed of 100 rpm; however, once Re > 20000, the pressure drag decreased along with the overall C_D on the cylinder. Larger inertial effects from the rough surface seemed to delay the flow separation behind the cylinder, resulting in a smaller wake, which in turn, reduced the drag and the drag coefficient. For conclude the results compiled, physically the graph shows a similar shapes with a rotation speed 0 rpm, 100 rpm and 400 rpm. However its shown a slightly different in C_D at certain location on the cylinder where's proportional with a Re>15000.

The lift coefficient (C_L) of the non-rotating and rotating cylinder was calculated for each type of surface roughness, displayed in Fig. 7(a), (b) and (c). When Re < 20000, the rotational rate in the counter-clockwise direction with speed of 100 rpm and 400 rpm yielded an insubstantial difference in the lift coefficient. It is observed that the lift predicted by the rotating cylinder is vastly different compared to the non-rotating cylinder. Lift performance may have been altered due to the dominance of the vortices created by rotation over the inertial forces of the flow. It was discovered that when the surface roughness was higher (cylinder D), there was a small reduction in the lift force. Swing of the wake was evident when the rough cylinder caused turbulence. It seemed that an earlier transition in the critical phase resulted when the Reynolds number was low (Re < 20000). However, when the Reynolds number increased (beyond Re > 20000), a significant rise in the fluctuating lift was noted when an on-going turbulence intensity and increased roughness was present. The experiment proved that rotation had an insignificant effect on the lift when Re > 20000 since the inertial forces became more dominant than the vertical effects originating from rotation.

It was observed that the regional effect of each type of surface cylinder roughness was significant in the increase of the fluctuation lift. The effect of surface roughness on the aerodynamic damping was identical to the effect of increasing turbulence intensity in the subcritical regime, as stated by Cheung and Melbourne[32]. As Reynolds number increased (Re >20000), the surface roughness on aerodynamic damping decreased.

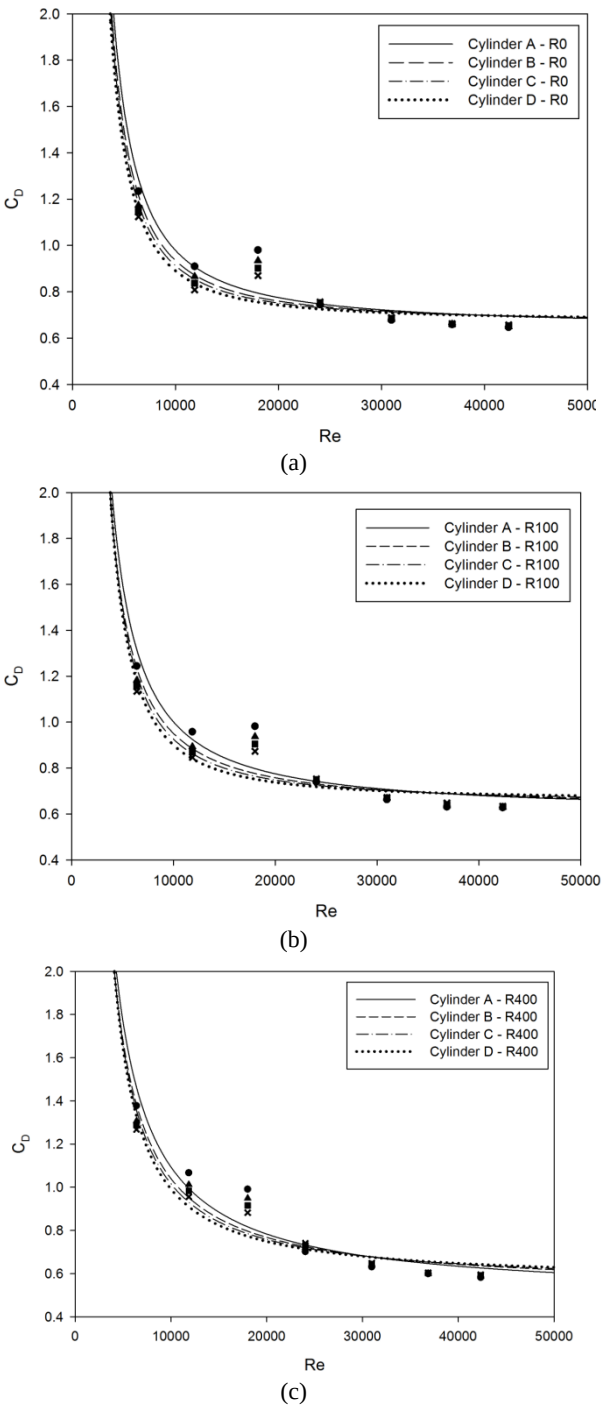

Fig.6 - C_D for cylinder with different roughness (a) C_D at 0 rpm (b) C_D at 100 rpm (c) C_D at 400 rpm.

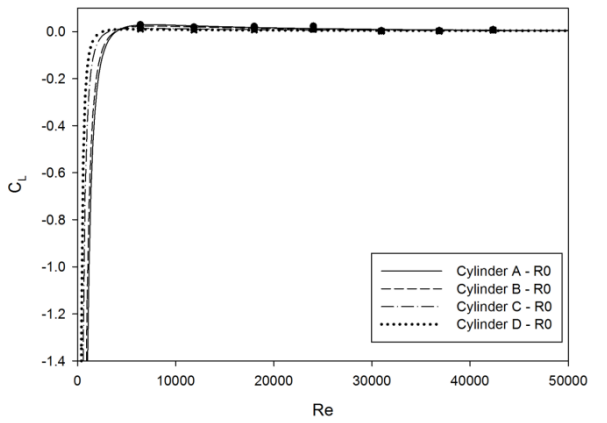

(a)

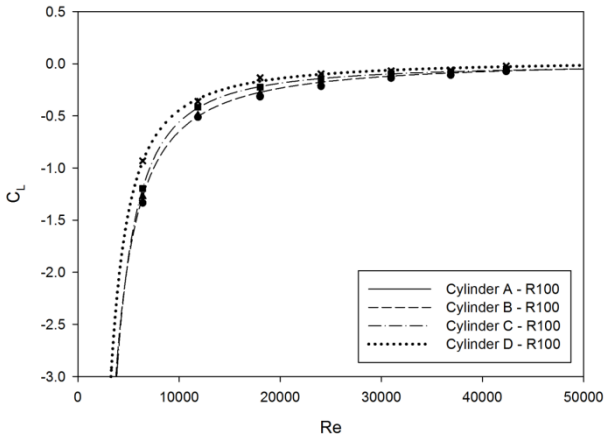

(b)

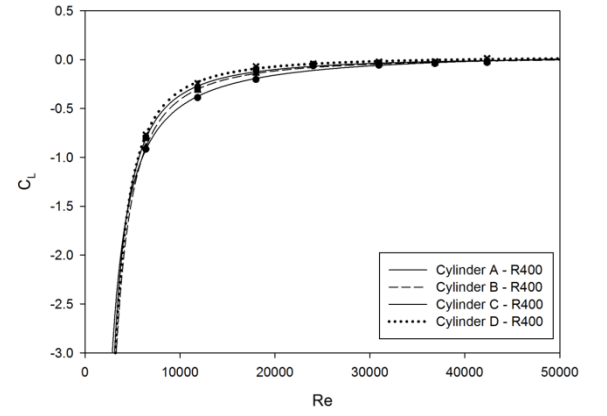

(c)

Fig.7 - C_L for cylinder with different roughness (a) C_L at 0 rpm (b) C_L at 100 rpm (c) C_L at 400 rpm.

The considerable amounts of force (with various proportion and direction) exerted by the flow over a rotating cylinder usually determines the ability of the air velocity to stay connected to the rough cylinder, in contrast to the loads produced in non-rotating cases. The nature of C_D was presented as shown in Fig 8 and 9) that represented the varied roughness, each with a speed range of 0-400 rpm and air velocity ($2000 \leq Re \leq 42000$, corresponding to 0.65 – 13.21 m/s). When the Reynolds number was decreased ($2083 \leq Re \leq 11859$), the C_D value would distinctly decrease initially and then increase a little before staying constant. This was the case for all four cylinders with varied surface roughness. Drag performance was marginally influenced by the cylinder speed (rpm). This was in accordance to D.W Moore's[33] theory that the drag coefficient was not affected by the cylinder rotation when speed was a substantial value.

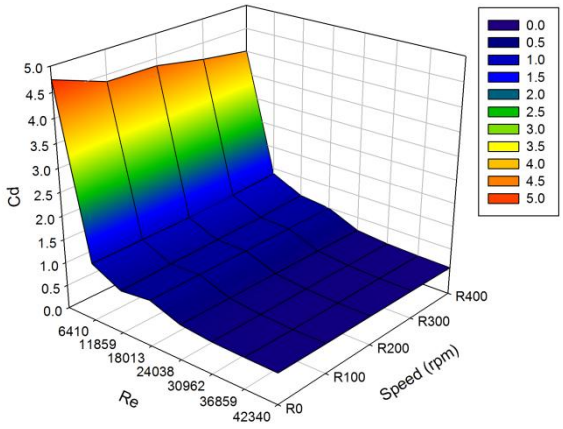

Cylinder A

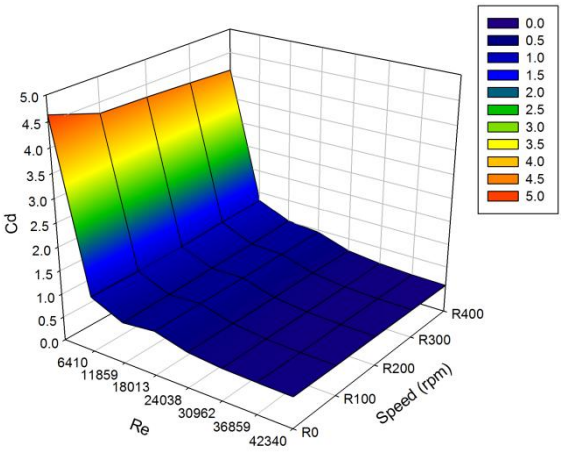

Cylinder B

Fig.8 - Drag maps of various roughness as function of *Re* and cylinder speed (rpm)-Cylinder A and B

Conclusions

The accomplishment of the LWSM was favourable since it easily attached to the wind tunnel, provided dynamic functions, minimised vibrations and accurately measured the lift and drag forces.

Due to surface roughness, there was a delay of flow separation behind the cylinder which decreased the difference in pressure between the areas before and after the circular cylinder. This

led to the conclusion that drag coefficients of rough surfaces were lower than those of smooth surfaces.

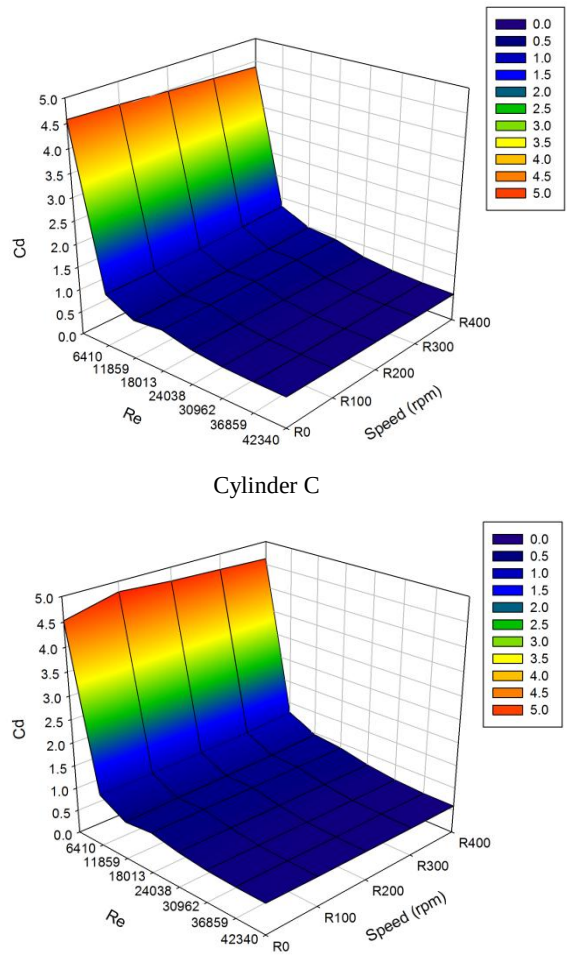

Cylinder C

Cylinder D

Fig.9 - Drag maps of various roughness as function of *Re* and cylinder speed (rpm)-Cylinder C and D

The rotational speed (ranging between 0-400 rpm) of the cylinder distinctly affected the lift performance, more so than the drag coefficient which was hardly influenced. During rotation, forces such as the torque and the Magnus effect were produced, causing an increased lift to the cylinder. The vertical take-off landing (VTOL) normally actualise this function on aircrafts.

The primary justification for the considerable reduction of the lift and drag forces may have been due to the range of the surface roughness on the cylinder, resulting in a near-wake flow formation that trailed the cylinder; which, in turn, postponed the vortex construction and the position of the vortex shedding.

Acknowledgement

Authors gratefully acknowledge the sponsorship and support from the Higher Ministry of Education and Department of Mechanical Engineering, Politeknik Seberang Perai, Penang, Malaysia. Thanks are also due to Mr. Azhar Ahmad, for their valuable assistance in the experiment.

References

1. This journal is a referred from the literature on studies and work: e.g.; P.W. Bearman, Vortex shedding from oscillating bluff bodies, *Ann. Rev. Fluid Mech*. 16 (1984) 195–222.
2. E. Naudascher, Flow-induced streamwise vibrations of structures, J. *Fluids Struct*. 1 (1987) 265–298.
3. M. Griffin, M.S. Hall, Review; Vortex shedding lock-in and flow control in bluff body wakes, *ASME J. Fluids Eng*. 113 (1991) 526–537.
4. A. Okajima, H. Takata, T. Asanuma, Viscous flow around a rotationally oscillating circular cylinder, *Report of Inst. Space Aero. Sci., University of Tokyo*, 1975, No. 532, 311–318.
5. J.R. Filler, P.L. Marston, W.C. Mih, Response of the shear layers separating from the circular cylinder to small amplitude rotational oscillations, *J. Fluid Mech*. 231 (1991) 481–499.
6. N. Fujisawa, K. Ikemoto, K. Nagaya, Vortex shedding resonance from a rotationally oscillating cylinder, *J. Fluid Struct*. 12 (1998) 1041–1053.
7. N. Fujisawa, Y. Kawaji, K. Ikemoto, Feedback control of vortex shedding from a circular cylinder by rotational oscillations, *J. Fluid Struct*. 15(2001) 23–37.
8. P.T. Tokumaru, P.E. Dimotakis, Rotary oscillation control of a cylinder wake, *J. Fluid. Mech*. 224 (1991) 77–90.
9. Mittal, S., Kumar, B., 2003. Flow past a rotating cylinder. *Journal of Fluid and Mechanics* 476, 303-334
10. Rao, A., Stewart, B.E, Thompson, M.C., Leweke, T., Hourigan, K., 2011. Flows past rotating cylinders next to a wall. *Journal of Fluids and Structures* 27, 668-679
11. Paluri Satish, Saurabh S. Patwardhan, O.N. Ramesh., 2013. Effect of steady rotation on low Reynolds number vortex shedding behind a circular cylinder. *Journal of Fluids and Structures*.
12. F.Gu, J.S. Wang, X.Q, Qiao, Z. HUANG, 2012. Pressure distribution, fluctuating forces and vortex shedding behavior of circular cylinder with rotatable splitter plates. *Journal of Fluids and Structure*. 28, 263-278.
13. K.M. Lam, Vortex shedding flow behind a slowly rotating circular cylinder. *Journal of Fluids and Structures*. 26(2009) 245-262.
14. Jones.G.W., Cincotta, J.J. Walker, R.W. 1969. Aerodynamics forces on a stationary and oscillating circular cylinder at high Reynolds numbers. *NASA Tech. Rep*. R-300.
15. Achenbach, E. 1977. Heat transfer and flow around a circular cylinder with tripping-wires. *Int. J. Heat Mass Transfer* 20, 359.

16. Y. Nakamura and Y. Tomonari.,1982. The effect of surface roughness on the flow past circular cylinder at high Reynolds numbers. *J. Fluid Mech*. Vol.123, PP. 363-378.
17. Farivar, D., 1981. Turbulent uniform flow around cylinders of finite length. *AIAA Journal* 19, 275–281.
18. Shedden, R., Lin, S.P., 1983. Drag-force fluctuation on a cylinder. *Journal of Fluid Mechanics* 127, 443–452.
19. Sakamoto, H., Oiwake, S., 1984. Fluctuating forces on a rectangular prism and a circular cylinder placed vertically in a turbulent boundary layer. *ASME Journal of Fluids Engineering* 106, 160–166.
20. So, R.M.C., Savkar, S.D., 1981. Buffeting forces on rigid circular cylinders in cross flows. *Journal of Fluids Mechanics* 105, 397–425.
21. Sin, V.K., So, R.M.C., 1987. Local force measurement on finite span cylinders in a cross-flow. *ASME Journal of Fluids Engineering* 109, 136–143.
22. Baban, F., So, R.M.C., O. tu.gen, M.V., 1989. Unsteady forces on circular cylinders in a cross flow. *Experiments in Fluids* 7, 293–302.
23. Baban, F., So, R.M.C., 1991. Aspect ratio effect on flow-induced forces on circular cylinders in cross-flow. *Experiments in Fluids* 10, 313–321.
24. Fox, T.A., West, G.S., 1993a. Fluid-induced loading of cantilevered circular cylinders in a low-turbulence uniform flow. Part 1: mean loading withaspect ratios in the range 4–30. *Journal of Fluids and Structures* 7, 1–14.
25. Fox, T.A., West, G.S., 1993b. Fluid-induced loading of cantilevered circular cylinders in a low-turbulence uniform flow. Part 2: fluctuating loads on a cantilever of aspect ratios 30. *Journal of Fluids and Structures* 7, 15–28.
26. West, G.S., Apelt, C.J., 1997. Fluctuating lift and drag forces on finite lengths of a circular cylinder in the subcritical Reynolds number range. *Journal of Fluids and Structures* 11, 135–158.
27. K. Lam, F. H. Wang, J.Y. Li, R.M.C. So., 2004. Experimental investigation of the mean and fluctuating forces of wavy (varicose) cylinders in a cross-flow. *Journal of Fluids and Structures* 19,321–334
28. K.M. Lam, Vortex shedding flow behind a slowly rotating circular cylinder. *Journal of Fluids and Structures.* 26(2009) 245-262.
29. C. Badalamenti, S. A. Prince, Vortex Shedding From a Rotating Circular Cylinder at Moderate Sub-Critical Reynolds Numbers and High Velocity Ratio. *26th International Congress of The Aeronautical Sciences, City University, London, UK*. (2008).
30. U. Butt and C. Egbers, 2013. Aerodynamic characteristics of flow over circular cylinders with patterned surface. *International Journal of Materials, Mechanics and Manufacturing* V1.27
31. Achenbach, E. 1977. Heat transfer and flow around a circular cylinder with tripping-wires. *Int. J. Heat Mass Transfer* 20, 359.
32. Cheung, J.C.K., Melbourne, W.H. Turbulence effects on some aerodynamic parameters of a circular cylinder at supercritical Reynolds numbers. *J. Wind Eng. Ind. Aerodynamic.* 14, (1983), 399–410.
33. D.W Moore, The flow past a rapidly rotating circular cylinder in uniform stream. *J. Fluids Mech.* 2, 541 (1957).